Klaus Dolling[1], Elizabeth Ritchie and Scott Tyo
University of Arizona

1. Introduction

The large differences in size and strength of tropical cyclones (TCs) result in considerable variability in their impacts on both marine interests at sea and inhabited coastal areas during close approach and landfall. Larger storms may have increased storm surge, increased oceanic upwelling, and a wider area in which flooding and damaging winds may occur as well as a larger area of rainfall. Thus a robust and accurate depiction of the extent of damaging winds is important both to directly prepare for impacts and also to properly initialize numerical weather prediction (NWP) forecasts of future TC motion, intensity, and wind structure. The size of a TC also has important implications for TC bogusing techniques. The insertion of a synthetic bogus vortex into a model is used extensively (Leslie and Holland 1995; Pu and Braun 2001; Kwon et al. 2002; Kwon and Cheong 2010), and knowledge of TC size in the data-sparse oceans would be useful in customizing the bogused vortex for individual models.

Operational centers, including the National Hurricane Center (NHC), the Joint Typhoon Warning Center (JTWC), and the Japan Meteorological Agency (JMA), among others, routinely provide forecasts of the wind field structure of active TCs within their area of responsibility. Forecasts of the wind radii, representing the maximum radial extent of the 34-, 50-, and 64-kt (1 kt = 0.52 m s^{-1}) winds (hereafter referred to as R34, R50, and R64 respectively) in 4 quadrants circling the TC (northeast, southeast, southwest, and northwest quadrants) are routinely constructed.

The current study extends research based on the deviation angle variance (DAV) technique (Piñeros et al. 2008), which utilizes digital brightness temperatures from long-wave infrared (IR) satellite images to objectively measure the symmetry of a TC solely based on a comparison of the gradient vectors of brightness temperatures from an actual TC with the gradient vectors of an ideal, symmetric vortex. The DAV technique has already been utilized to obtain TC intensity and as a means of identifying cyclogenesis in the Atlantic, eastern North Pacific, and western North Pacific basins (Ritchie et al. 2012; Ritchie et al. 2013; Wood, 2012) In this study, the spatial-temporal structure of the DAV signal for TCs is utilized (Piñeros et al. 2010) along with wind radii from the Extended Best Track and information from the Statistical Hurricane Intensity Prediction Scheme (SHIPS) model (DeMaria and Kaplan 1994; 1999; DeMaria et al. 2005) to provide a multiple linear regression technique that objectively calculates the wind radii for a given
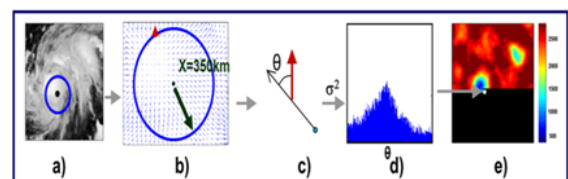

Figure 1. Map of deviation-angle variances: (a) IR image. The area analyzed around a reference point is indicated by the black circle (350 km); (b) gradient field of the brightness temperatures within the circle in (a); (c) Deviation-angle calculation for (black arrow) a gradient vector relative to a radial line extending from the reference point; (d) Deviation-angle histogram; and (e) Map of deviation-angle variances [deg^2]. (adapted from Piñeros et al. 2010).

[1] Corresponding author: K. Dolling, Department of Atmospheric Sciences, University of Arizona, 1118 East 4th St, Tucson, AZ 85721-0081
dolling@atmo.arizona.edu

TC on a half hourly basis. The results from the technique presented here are tested against TCs with aircraft reconnaissance occurring within 3 hr of a Best Track estimate. A model is produced that predicts the symmetric and asymmetric components of the wind radii on a half-hourly basis. The model will provide objective wind field estimates in real-time that may be used by forecasters and NWP model initialization.

2. Data and Methodology

The data used for this study are digital brightness temperatures from long-wave (10.7 μm) IR satellite images. Approximately 4,708 half-hourly images from the Geostationary Operational Environment Satellite 12 (GOES 12) imager are processed from 21 TCs for the years 2004-2010 in the North Atlantic basin. Tropical cyclones are chosen based on the occurrence of aircraft reconnaissance within 3 hr of a best track time. For the purposes of the regression, each case required at least 48 hr of semi-continuous reconnaissance, so they are confined to the Atlantic basin west of 55˚ W where aircraft reconnaissance is routinely performed. Following the methodology of Piñeros et al. (2010), the deviation angles at each pixel within a 500-km radius of the central reference point were computed. The sensitivity to different radii for the DAV calculation was tested; the 500-km radius was determined to provide the best relationship with the wind radii. The variance of the histogram of deviation angles was calculated and mapped back to the reference pixel in order to create the map of variances for that satellite image (Fig. 1). For more information on the DAV and its use in TCs, see Piñeros et al. (2008, 2010, 2011).

In the present study, a map of DAV is calculated for each half-hourly satellite image for the entire time in which the TC had reconnaissance data. A multiple linear regression technique is developed to model both the symmetric and axisymmetric parts of the wind radii. Variables from the best track data, and environmental parameters from the SHIPS model are utilized in
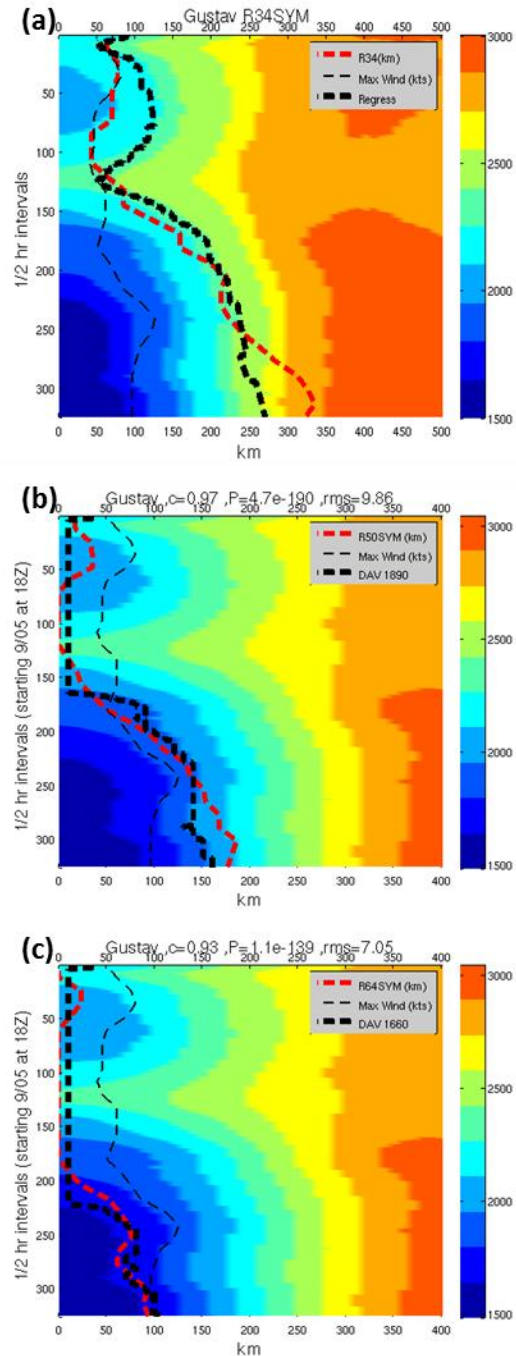

Figure 2. *Hovmoller diagram of the azimuthally-averaged DAV signal plotted in color shading with values corresponding to the color bar on the right for tropical cyclone Gustav. The red dashed line is the symmetric observed wind radii (km) and the thick black dashed line displays the regression line (km). The thin black dashed line displays the intensity of the TC in kts. (a) 34 kt winds. (b) 50 kt winds. (c) 64 kt winds. The thin black dashed line is the TCs intensity in kts.*

the regression model. The preliminary step plots each TC with the azimuthally averaged DAV signal for each radius along with the symmetric component of the Extended Best Track wind radii using the Best Track centers. After all the data are processed, the DAV signals with the lowest root mean squared error (RMSE) corresponding to each of the three wind radii are used in the regression model. The next step consists of a screening regression known as forward selection (Wilks 2006). Each of the predictors is numerically tested for the strength of their linear relationship to the predictand. After the predictor with the best linear relationship to the predictand is selected, the process is repeated with the remaining variables. This continues until the predictors display diminished improvements within the regression equation. Once the predictors improve the regression equation by less than 1%, they are ignored. TC age, SSTs, and maximum wind speed are the best predictors for both the symmetric and asymmetric models (Table 1).

Wind Radii	MAE	R^2	P-Value	Predictors
R34	20.8	0.72	0	DAV, TC age, SST
R50	12.5	0.79	0	DAV, TC age, SST
R64	7.3	0.84	0	DAV, TC age, Max Wind

Table 1. Results from the multiple linear regressions. First column is the wind radii (kts). Second and 3rd column are the mean absolute error (n mi) and R^2 values. Forth and 5th columns display the P-value and the predictors used for each radii.

The large sample size (4,708 half hourly satellite images) is ideal for the statistical testing of the data. A cross-validation method is used to investigate the forecast precision of the wind radii. Using this method, 80% of the data are used to create the multiple linear regression parameters, and the linear regression model is then tested on the remaining 20% of the data. This method is applied 5 times by leaving out successive 20% increments of data and using

the other 80% to create the multiple linear regression models. The method is used for both the symmetric and the asymmetric calculations of the different wind radii.

3. Results

Table 1 displays the wind radii, the MAE, R^2 values, P values and the best linear predictors. For the symmetric regression, adding more than 2 predictors yielded negligible returns, thus only the top two predictors besides the DAV were used. In addition to the DAV signal, TCage was the largest contributor to the relationship for all cases. The multiple linear regression model produces estimates for the wind radii with MAEs of 20.8, 12.5, and 7.3 n mi for R34, R50, and R64 respectively. P-values in all cases have confidence levels above the 99.9% confidence level indicating a strong relationship between the predictors and the predictand.

Figure 2 displays the symmetric components of the R34, R50, and R64 respectively for Hurricane Gustav. Hurricane Gustav is a good example of a TC that varies in both intensity and the size of the wind radii through its sample period. In each of the panels, the DAV signal closely mimics the shape of the wind field. The added predictors increase this accuracy.
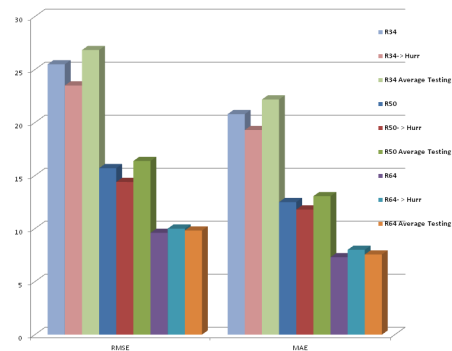

Figure 3. Chart displaying the root mean square error (RMSE) and the mean absolute error (MAE) for the R34, R50, and R64 kt wind radii. Also included are the 3 radii with the stipulation that their intensity must be hurricane intensity or higher and the average of the 5 bins tested during the cross-validation analysis. Values are in nautical miles.
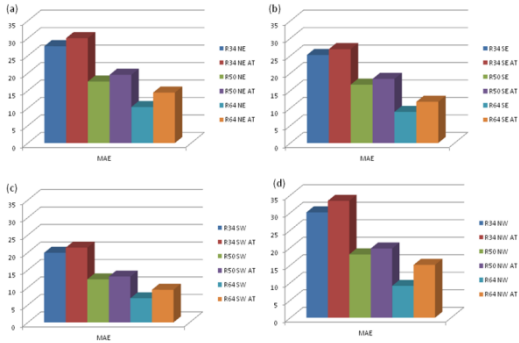
Figure 4. Mean absolute error (MAE, nm) for: (a) northeast; (b) southeast; (c) southwest; and (d) northwest quadrants of the R34, R50, and R64 kt wind radii. Also included are the average testing (AT) of the 5 bins from the cross-validation analysis.

To test the model over a larger dataset, a cross-validation method was utilized. The results are displayed in Figure 3 for all wind radii. Notice that the tests result in RMSE and MAE values that are similar to the "all data" regression model demonstrating that our model is consistent and produces similar results when forecasting for subsets of the data. R^2 values steadily increase from R34 to the R64, and p-values of each subset tested for all wind radii display confidence levels above 99.9%.
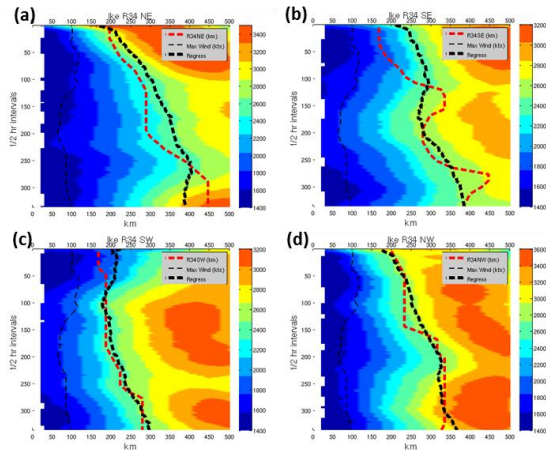

Figure 5. Test case using all tropical cyclones except Ike for the regression. All values are as in Fig.2 except for individual quadrants. The red dashed line is the symmetric 34 kt wind radii (km) and the thick black dashed line displays the regression line (km). The thin black dashed line is the TCs intensity in kts: (a) Northeast quadrant; (b) Southeast quadrant; (c) Southwest quadrant; and (d) Northwest quadrant.
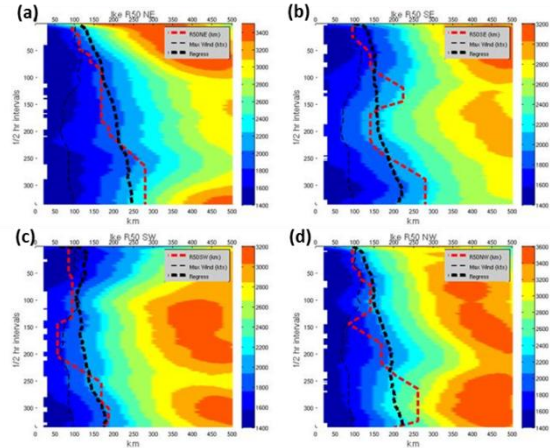

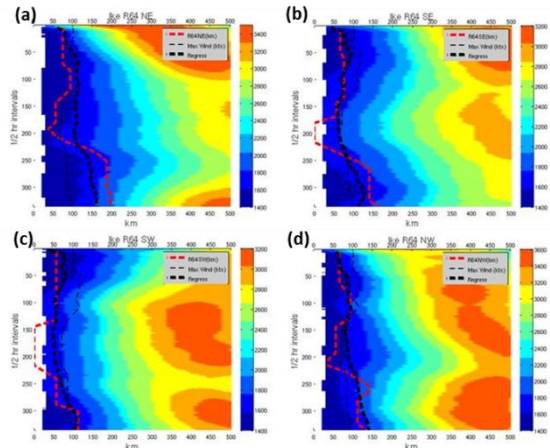**Figure 6.** Same as Figure 5 except for R50.

Figure. 7. Same as Figure 5 except for R64.

The results for the asymmetric analysis are listed in Figure 4. As mentioned above, the analysis utilizes the azimuthally averaged DAV from each TC quadrant. For each of the wind radii, the NE and NW quadrants have the highest MAE, yet when taken as a percentage of the average wind radius in each quadrant, they usually score lower than other quadrants. The SW quadrant consistently has the lowest MAEs, likely an artifact of the general motion of TCs to the east and north and the smaller average wind radii in that quadrant.

R^2 values for the cross-validation of the asymmetric regression all have confidence levels above the 99.9% level. In general the average testing of the intervals produces MAEs

which are a few points higher than the actual MAEs (Fig. 4).

As an added test to investigate the ability of the asymmetric regression model to estimate wind radii for TCs, the data from TC Ike are withheld and the regression parameters are derived from the remaining TCs. TC Ike remained above hurricane intensity for the entire observation period, therefore the regression model of hurricane intensity and above subset is used. As displayed in Figs. 5, 6, and 7 for R34, R50, and R64 respectively, the regression is able to model the general shape and distance of each wind radius in each quadrant, though the observed wind radii (i.e. Fig. 5b) display some large swings while the regression model tends to have a smoother shape to it.

A comparison of the wind structure between the DAV regression and the aircraft reconnaissance is displayed in Fig. 8. The DAV regression model captures the general shape and size of the vortex as reported by reconnaissance data.
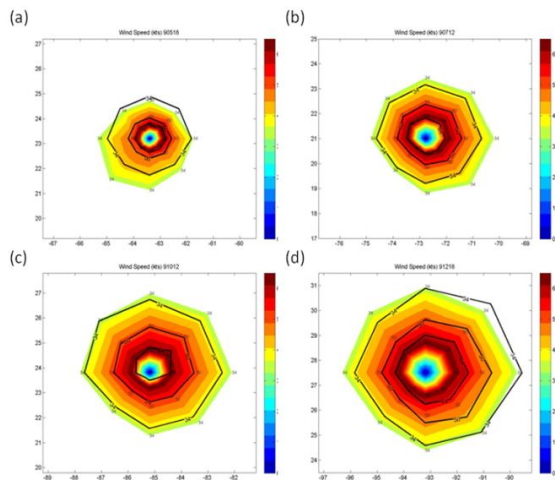

Figure 8. *Modeled DAV regression in color and black contours from aircraft data (3 contours are the 34, 50 and 64 kt wind radii at for Hurricane Ike over a 6 day period on (a) 09/05/08 at 18 UTC (b) 09/07/08 at 12 UTC (c) 09/10/08 at 12 UTC and (d) 09/12/08 at 18 UTC.*

4. Conclusions

Approximately 4,708 half-hourly images from GOES 12, brightness temperature images are processed from 21 TCs from the years 2004-2010 that had extensive in-situ observations. The current study extends past research based on the DAV that utilizes digital brightness temperatures from long-wave IR satellite images to objectively measure the symmetry of a TC solely based on a comparison of the gradient vectors of brightness temperatures from an actual TC with the gradient vectors of an ideal, symmetric vortex. Maps of the DAV with respect to time provide information on the symmetry of TCs. Lower DAV values are associated with higher symmetry and higher values with less symmetry. In this study the spatiotemporal information in these maps, along with information from Best Track and the SHIPS model, has been utilized to create a multiple linear regression model. This objective model is utilized to estimate the 34-, 50- and 64-kt wind radii.

Symmetric and asymmetric models are derived. The symmetric model produces MAEs of 20.8, 12.5, and 7.3 n mi for R34, R50, and R64, respectively. Confidence levels are above 99.9 % for all cases presented here. The asymmetric component of the wind radii are also modeled using azimuthally averaged DAV in the NE, SE, SW, and NW quadrants of the TC. Using the same predictors as the symmetric model gave the best estimates of the wind radii. MAEs for R34 in the NE, SE, SW, and NW quadrants are 27.7, 25.2, 19.9, and 30.1 n mi respectively. The MAEs for R50 for the same quadrants are 17.6, 16.7, 12.3, and 18.1 n mi. R64 has MAEs in each quadrant of 10.3, 8.9, 6.9, and 9.1 n mi. In the future the regression model will hopefully be useful in data sparse oceans with no aircraft reconnaissance to approximate the size and strength of TCs wind fields. Synthetic vortices created with this regression model may help generate a more realistic structure for the bogus vortex in NWP models which may

increase the accuracy of the track, intensity, rainfall, and surge forecasts.

References

DeMaria, M. and J. Kaplan, 1994: A statistical hurricane intensity prediction scheme (SHIPS) for the Atlantic Basin. *Wea. Forecasting*, **9**, 209-220.

_____, and _____, 1999: An updated statistical hurricane intensity prediction scheme (SHIPS) for the Atlantic and Eastern North Pacific Basins. *Wea. Forecasting*, **14**, 326-337.

_____, M. Mainelli, L. K. Shay, J. A. Knaff, and J. Kaplan, 2005: Further improvements to the statistical hurricane intensity prediction scheme (SHIPS). *Wea. Forecasting*, **20**, 531-543.

Kwon, I-H, H-B. Cheong, 2010: Tropical cyclone initialization with a spherical high-order filter and an idealized three-dimensional bogus vortex. *Mon. Wea. Rev*., **138**, 1344-1367.

Kwon, H. J., S-H. Won, M-H. Ahn, A-S. Suh, and H-S. Chung, 2002: GFDL-Type typhoon initialization in MM5. *Mon. Wea. Rev*., **130**, 2966-2974.

Leslie, L. M. and G. J. Holland, 1995: On the bogussing of tropical cyclones in numerical models: A comparison of vortex profiles. *Meteorol. Atmos. Phys*., **56**, 101-110.

Piñeros, M. F., E. A. Ritchie, and J. S. Tyo, 2008: Objective measures of tropical cyclone structure and intensity change from remotely-sensed infrared image data*. IEEE Trans.* Geosciences and remote sensing. **46**, 3574-3580.

Piñeros, M. F., E. A. Ritchie, and J. S. Tyo 2010: Detecting tropical cyclone genesis from remotely-sensed infrared image data. *IEEE Trans. Geosciences and Remote Sensing Letters*, **7**, 826-830.

Piñeros, M. F., E. A. Ritchie, J. S. Tyo, 2011: Estimating Tropical Cyclone Intensity from Infrared Image Data. *Wea. Forecasting*, **26**, 690–698.

Pu, Z. X., and S. A. Braun, 2001: Evaluation of bogus vortex techniques with four-dimensional variational data assimilation. *Mon. Wea. Rev*., 129, 2023-2039.

Ritchie, E. A., G. Valliere-Kelley, M. F. Pineros, and J. S. Tyo, 2012: Improved tropical cyclone intensity estimation using infrared imagery and best track data. *Wea. Forecasting*., **27**, 1264-1277.

_____, K. M. Wood, M. F. Piñeros, O. G. Rodriguez-Herrera, and J. S. Tyo, 2013: Estimating tropical cyclone intensity in the North Pacific Ocean using the deviation-angle-variance technique. *Wea. Forecasting. (In Press)*

Wilks, D. S., 1995. Statistical Methods in the Atmospheric Sciences. Academic Press, pp. 179-217.

Wood, K. M., 2012: Evaluating the impacts of eastern North Pacific tropical cyclones on North America utilizing remotely sensed and reanalysis data. Ph.D. dissertation, The University of Arizona.